

NMR Imaging of the Distribution of the Liquid Phase in a Catalyst Pellet during α -Methylstyrene Evaporation Accompanied by Its Vapor-Phase Hydrogenation

Igor V. Koptuyug,* Alexander V. Kulikov, Anna A. Lysova, Valery A. Kirillov, Valentin N. Parmon, and Renad Z. Sagdeev

International Tomography Center, 3A Institutskaya St., Novosibirsk 630090, Boreskov Institute of Catalysis, 5 Acad. Lavrentiev Pr., Novosibirsk 630090, and Novosibirsk State University, 2 Pirogova St., Novosibirsk 630090, Russia

Received April 29, 2002

Trickle-bed reactors are widely used in chemical industry. They can operate in various regimes, and under certain circumstances the development of critical phenomena is possible, potentially leading to the formation of local hot spots and thermal explosion. To achieve a safer and a more efficient process it is essential to undertake the fundamental studies of the distribution of the liquids and gases, phase transitions, and mass-transport processes in an operating reactor in situ. Only a few techniques can directly visualize the processes inside optically nontransparent reactors and catalyst grains in a noninvasive way under reactive conditions. Nuclear magnetic resonance (NMR) has a long and impressive history of applications to study chemical reactions. It is able to provide information on the chemical composition of a mixture, and thus to identify reactants, products and in some cases the intermediate species. The recognition that by spoiling the magnetic field homogeneity one can add spatial information to an NMR experiment eventually led to a wide-spread use of magnetic resonance imaging (MRI) as a valuable diagnostic tool in medicine. At the same time, while recognized, the potential of the MRI technique in nonmedical research and in particular in catalysis is yet to be appreciated and exploited. MRI can provide information on the distribution of liquids and gases in optically nontransparent porous solids.¹ Besides, pulsed field gradient (PFG) NMR and MRI are often used for studying mass transport of liquids, solids, and gases.¹ Therefore, the combination of various modalities of the NMR technique provides a unique opportunity to study a chemical transformation coupled to various mass-transport and phase-transition processes in situ in a catalytic reactor or in a single catalyst grain. The MRI studies of chemical reactions published to date predominantly deal with polymerization² and the Belousov–Zhabotinsky chemical oscillator.³ It appears that the only application in heterogeneous catalysis is the study of room-temperature esterification of methanol.⁴ To the best of our knowledge, the work reported below is the first example of the application of MRI to study a heterogeneous reaction which proceeds at an elevated temperature, namely the hydrogenation of α -methylstyrene (AMS) on a single grain of Pt/ γ -Al₂O₃ catalyst.

A cylindrical catalyst pellet (diameter and height 4.7 mm, specific surface area 194 m²/g, pore volume 0.65 cm³/g, pores with 4–8 nm radii account for 0.42 cm³/g; 15% Pt by weight) was placed inside the probe of a Bruker DRX-300 high-resolution NMR instrument equipped with the microimaging accessory. The slice-selective spin–echo technique¹ with ¹H NMR signal detection was employed to map the distribution of liquid within a 2-mm thick axial slice of the pellet with the in-plane spatial resolution of (230

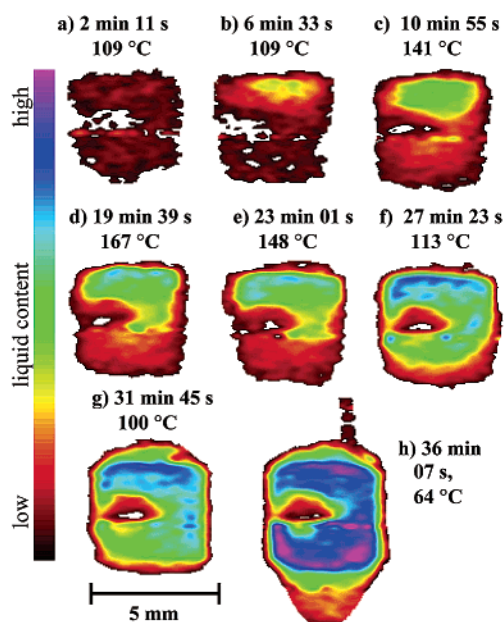


Figure 1. Spatial maps of the liquid phase in the catalyst pellet under reactive conditions. For each image, the temperature and the time of detection are indicated. The intensity scale is shown at the left-hand side.

$\times 140$) μm^2 . No attempt was made to minimize the acquisition time of each image (4 min and 22 s). A stream of hydrogen gas heated to 67–69 °C and saturated with AMS vapor was supplied to the pellet at a flow rate of 18.5 cm³/s. A thermocouple implanted into the pellet through its side (an area void of signal in the center of the pellet, Figure 1), indicated that the pellet temperature rose 40 °C above that of the gas due to the exothermic nature of the reaction. While no liquid was supplied to the pellet at this stage, Figure 1a nevertheless shows the presence of the liquid phase within the pellet, possibly due to the adsorption/condensation of AMS and the major product cumene within the pores. In our experimental setup, liquid AMS can be supplied to the top of the pellet via a capillary which can be seen in Figure 1h. The flow of AMS (0.43 $\times 10^{-3}$ g/s) was turned on simultaneously with the beginning of the detection of image 1b. This led to a substantial increase in the amount of liquid in the upper part of the pellet. The rugged edges of the area filled with liquid indicate an efficient evaporation of AMS, with the drying front residing within the pellet. AMS vapor reacts on the nonwetted surface inside the catalyst pellet, and the temperature rises to 167 °C (Figure 1d). During the detection of image 1d the flow rate of liquid AMS was increased to 0.57 $\times 10^{-3}$ g/s. This led to a new steady-state (Figure 1f) characterized

* To whom correspondence should be addressed. E-mail: koptuyug@tomo.nsc.ru

by a lower pellet temperature, a higher liquid content, and a shift of the evaporation/reaction region toward the lower edge of the pellet. The irregular shape of the liquid front observed in Figure 1 is in marked contrast to the smooth edges of the liquid-filled area observed in the absence of reaction when no hydrogen gas is supplied (results not shown). Further increase of liquid AMS flow rate to 0.71×10^{-3} during the detection of image 1g led to the complete saturation of the porous pellet with the liquid, formation of the droplet of liquid below the pellet, and a small dome on top of it (Figure 1h). The endothermic evaporation of the liquid phase becomes prevalent, and the pellet temperature drops slightly below the temperature of the surrounding gas.

Several experiments were performed with the hydrogen gas containing no AMS vapor. As demonstrated earlier by the indirect studies of AMS hydrogenation that were based on the pellet temperature measurements with several implanted thermocouples,⁵ the reaction exhibits more than one steady-state regime, depending on the initial conditions and the liquid AMS flow rate. The lower branch of the hysteresis curve is characterized by the pellet temperature which is lower than the gas temperature and can be reached by starting with a dry pellet and using a relatively high liquid flow rate (pellet temperature 54 °C). The steady state on the upper branch of the hysteresis curve is reached by first flooding the pellet completely and then reducing the AMS flow rate, with the pellet temperature being higher (92–102 °C) than that of the gas. Both regimes have been achieved experimentally, and the distributions of liquid within the pellet have been mapped. In all cases, during a steady state the pellet temperature was stable within a few degrees,⁵ and the liquid distribution did not change.

The results obtained demonstrate that under conditions of the simultaneous evaporation of the reactant and the hydrogenation of its vapor, two regions with very different liquid content can form within the catalyst, with one region having large liquid content and the other one filled with the reacting gas–vapor mixture. The position of the evaporation area which separates the two regions depends on the specific experimental conditions. The single-grain arrangement can be considered as a simplified reactor design suitable for isolating and studying various individual regimes of its operation. The information obtained will help rationalize the behavior of a granular bed reactor since the redistribution of liquid within the bed is governed by the grain-wetting processes.

No attempt was made in this work to distinguish the reactant and product in the images obtained. NMR is able to distinguish different molecular species and even groups of atoms on the basis of the differences in their chemical shifts in NMR spectra. However, the NMR lines of molecules interacting with solid surfaces are known to be broadened due to the shortening of their nuclear spin relaxation times. For porous solids with large surface-to-volume ratios such broadening can exceed 3 orders of magnitude making the separation of the reactant and product contributions impossible. It is likely, however, that an NMR experiment performed without spatial resolution can exaggerate the line width problem. To demonstrate this, the same catalyst pellet was presoaked in a 1:1 mixture of AMS and cumene. Figure 2c shows the NMR spectrum of this sample detected at room temperature. The lines are clearly much broader than those of the bulk liquid (Figure 2a). While the contribution of the CH₂ group of AMS can be recognized at 5.2 ppm, the presence of a broadened and distorted line of the phenyl ring at 7.3 ppm makes the quantification of the mixture composition hardly possible. However, the detection of the NMR spectra with spatial resolution has demonstrated that the magnetic field within the sample is inhomogeneous. This inhomogeneity cannot be corrected with the standard shimming procedures employed in NMR

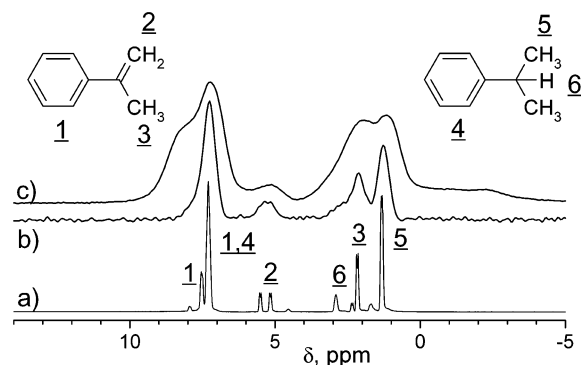


Figure 2. Proton NMR spectra of a 1:1 mixture of AMS and cumene detected for bulk liquid (a) and liquid permeating the catalyst pellet (b,c). Spectrum (b) was detected with spatial resolution. The number of acquisitions was eight (a,c) or two (b).

and is caused by the finite sample size and the mismatch of the magnetic susceptibilities between the sample and its surroundings. An example of the spatially resolved NMR spectrum is shown in Figure 2b. Since the spectrum corresponds to a volume of $(2 \times 0.5 \times 0.12) \text{ mm}^3$ which is much smaller than the characteristic length scale of the field inhomogeneity, the NMR lines of the spectra obtained for any location within the sample exhibit much narrower and less distorted lines, and the quantification of the mixture composition becomes possible. In this example, the ratio of the integrals of the two broadened lines at 7.3 and 5.2 ppm (Figure 2b) is 5.2, which is in agreement with the expected ratio of 10:2 for the 1:1 mixture. Thus, chemical shift imaging can be employed to disentangle the spatial distributions of the reactant and product. Besides, spin relaxation times of AMS and cumene within the pellet are different which provides an alternative way to distinguish the two species. We are currently exploring these possibilities.

Finally, a word of caution is in order. The gradient coils of the NMR imaging accessory can be damaged easily even by a moderate overheating (above 50–60 °C in our case). In our setup, a nonsilvered glass dewar protected the coils and the magnet bore from the warm air and gas (69 °C) and from the heat released due to the reaction (pellet temperatures up to 185 °C).

Acknowledgment. This work was supported by the Russian Foundation for Basic Research (Grants 02-03-32770 and 00-15-97450) and the Siberian Branch of the Russian Academy of Sciences (Integration Project No. 46). A.A.L. gratefully acknowledges a scholarship awarded by the Zamaraev International Charitable Scientific Foundation.

References

- (1) Callaghan, P. T. *Principles of Nuclear Magnetic Resonance Microscopy*; Clarendon: Oxford, 1991.
- (2) (a) Ahuja, S.; Dieckman, S. L.; Gopalsami, N.; Raptis, A. C. *Macromolecules* **1996**, *29*, 5356. (b) Wallin, M.; Glover, P. M.; Hellgren, A.-C.; Keddie, J. L.; McDonald, P. J. *Macromolecules* **2000**, *33*, 8443. (c) Nunes, T. G.; Pires, R.; Perdigo, J.; Amorim, A.; Polido, M. *Polymer* **2001**, *42*, 8051.
- (3) Su, S.; Menzinger, M.; Armstrong, R. L.; Cross, A.; Lemaire, C. *J. Phys. Chem.* **1994**, *98*, 2494. (b) Gao, Y.; Cross, A. R.; Armstrong, R. L. *J. Phys. Chem.* **1996**, *100*, 10159. (c) Cross, A. L.; Armstrong, R. L.; Gobrecht, C.; Paton, M.; Ware, C. *Magn. Reson. Imaging* **1997**, *15*, 719.
- (4) Gladden, L. F. *Abstracts of Papers*; 6th International Conference on Magnetic Resonance Microscopy, Nottingham, UK, 2001.
- (5) Slin'ko, M. G.; Kirillov, V. A.; Kulikov, A. V.; Kuzin, N. A.; Shigarov, A. B. *Dokl. Chem.* **2000**, *373*, 359.

JA026713U